

Spacecraft Electric Propulsion—An Overview

M. Martinez-Sanchez*

Massachusetts Institute of Technology, Cambridge, Massachusetts 02139

and

J. E. Pollard†

The Aerospace Corporation, El Segundo, California 90245

A short review of the status of electric propulsion (EP) is presented to serve as an introduction to the more specialized technical papers also appearing in this Special Issue (*Journal of Propulsion and Power*, Vol. 14, No. 5, Sept.–Oct. 1998). The principles of operation and the several types of thrusters that are either operational or in advanced development are discussed first, followed by some considerations on the necessary power sources. A few prototypical missions are then described to highlight the operational peculiarities of EP, including spacecraft interactions. We conclude with a historical summary of the accumulated flight experience using this technology.

I. Introduction

THIS paper is intended to serve as a general overview of the technology of electric propulsion (EP) and its applications, and to lead the interested reader to the more specific technical papers on the topic that are also included in this Special Issue. It is hoped that this series of papers will be of use not only to the propulsion specialist, but also to spacecraft (S/C) designers seeking to familiarize themselves with a technology that is now seeing rapid introduction.

EP is by no means a new concept, having first been tested in flight in the 1960s. However, its introduction as a practical alternative to chemical thrusters for S/C propulsion has been slow in developing, owing to a combination of insufficient onboard electrical power on most S/C, and a reluctance by many mission planners to abandon tried and true solutions. The potential performance advantage of primary EP for space missions with large ΔV requirements was recognized from the beginning, and much of the early research and development work addressed this type of mission. Yet, it has been the gradual application of the simpler forms of EP to secondary propulsion tasks that has led to its acceptance, with the long-envisioned deep-space applications only now beginning to materialize.

We first review the existing and emerging types of EP devices and their power sources, with some comments about their relative position in the mission spectrum. The missions themselves are examined to highlight the differences in planning that EP introduces. This is amplified in a brief review of the new S/C integration issues brought about by these thrusters. A summary is included of the flight experience accumulated up to the present time.

II. EP Systems

An EP system is a set of components arranged so as to eventually convert electrical power from the S/C power system into the kinetic energy of a propellant jet.¹ Figure 1 shows in schematic form the principal elements of an EP system and its interfaces with other S/C systems. Typically, the power system supplies regulated dc bus power to a power processor unit (PPU), as well as to other auxiliary elements, such as valves,

heaters, etc. The PPU processes this raw power into the specific form required by the thrusters and is usually one of the most complex and challenging EP components, as will be seen in subsequent sections. A regulated, pressure-fed fuel system is shown for illustration, although simple blowdown supplies can sometimes be used. No detail is shown of the plumbing, which often includes series and parallel valves, pyrotechnically opening or closing valves, etc. The flows to be handled are usually very small, but occur for very prolonged periods of time (months), which presents special challenges for the design of precise flow controllers and leak-free valving. Commands to the various power switches, valves, etc., are supplied by the S/C computer, which also receives and processes a variety of status signals from sensors (only a pair of pressure signals are illustrated).

The heart of the system is, of course, the thruster itself, and this paper will concentrate on thrusters. It must be understood, however, that a large proportion of the propulsion engineer's effort must be devoted to the balance of the EP system, which in the end is also usually heavier, bulkier, and more expensive than the thruster(s). Fortunately, aside from the PPU peculiarities, the rest of the system is not drastically different from more familiar cold-gas or monopropellant systems, and indeed, EP has benefited in its gradual introduction from this existing experience base.

III. Electric Thrusters

The common feature of all EP schemes is the addition of energy to the working fluid from some electrical source. This has been accomplished, however, in a large variety of physically different devices. Operation can be steady or pulsed; gas acceleration can be thermal, electrostatic, electromagnetic, or mixed; the propellant can be a noble gas, a chemical monopropellant, or even a solid. Of the many combinations tested over the years, a reduced, but still large number have reached maturity, or are approaching it. These are listed in Table 1, where a few of their principal attributes are also given. Simplified schematics of these thrusters are shown in Fig. 2 to illustrate their operating principles. The numerical values listed in Table 1 are not to be taken as recommended design values, but only as indicative of a range; for more detailed information, the reader is referred to the quoted literature.^{2–20}

A. Resistojets

As indicated in Fig. 2a, resistojets operate by passing the gaseous propellant around an electrical heater (which could be the inside of tubes heated radiatively from the outside), then

Received March 3, 1998; revision received June 15, 1998; accepted for publication June 24, 1998. Copyright © 1998 by the American Institute of Aeronautics and Astronautics, Inc. All rights reserved.

*Professor, Department of Aeronautics and Astronautics.

†Senior Scientist, Technology Operations.

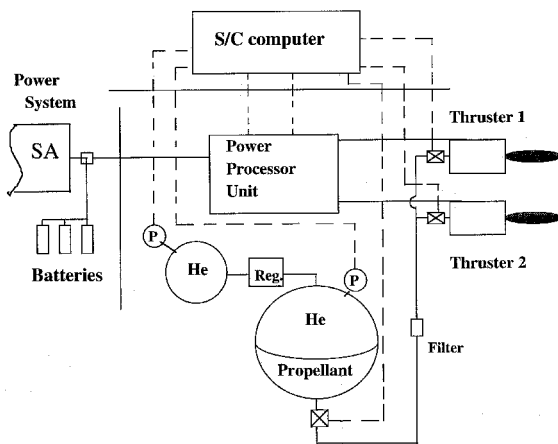


Fig. 1 Schematic of a typical EP system.

using a conventional nozzle to generate thrust. The heating reduces the gas flow rate from a given upstream pressure through a given nozzle area, thus leading to the familiar increase in specific impulse as \sqrt{T} . Nearly any gas could be used (as long as it is compatible with the high-temperature heater), and this may be dictated by considerations such as waste disposal on manned S/C. The most successful application has been based on the superheating of catalytically decomposed hydrazine, which has the advantage of commonality with familiar fuel systems used in hydrazine monopropellant applications. The heaters can operate over the wide pressure range encountered with blowdown systems, and their input voltage is low enough to require no special power conditioning, except for current surge protection. An exception to this would be a S/C power system that would allow more than about 20% voltage variations, in which case a dedicated regulator would become necessary. Operation can continue in a nonsuperheated mode in case of heater failure. The plume is not ionized and poses no unusual S/C interaction problems.

Because the molecular mass of the gas ($N_2/H_2/NH_3$) is relatively high, and because the heating wall is limited by materials (W-Re or something similar) to about 2000 K, the specific impulse (I_{sp}) achieved is only modest, of the order of 300–310 s. This is 40% better than that without superheating, and the improvement comes at a very small cost in complexity, if power is available. A favorable situation (for this and also for other EP techniques) occurs in geostationary communications satellites, in which excess power is indeed available most of the time (Sec. V), and this prompted the early commercial introduction of hydrazine resistojets (starting with Intelsat V, 1980) for the north-south stationkeeping (NSSK) function. A more recent application is for orbit insertion, control, and deorbit of the Iridium low Earth orbit (LEO) constellation. One of the few technical problems posed by these thrusters is the tendency of the hydrazine to produce nonvolatile deposits at the hot inlet to the catalytic chamber; this is common to all hydrazine thrusters, but the problem is made more critical by the reduction in flow rate because of the higher I_{sp} . Solutions have included the use of ultrapure hydrazine and thermal shunts to reduce heat flux at the critical points.

Ammonia resistojets have also been used for higher specific impulse (lighter gas), at some cost in complexity.

As shown in Table 2, resistojets have flown on Intelsat V, Satcom 1-R, GOMS, Meteor 3-1, Gstar-3, and Iridium S/C, in addition to some older satellites and test flights.

B. Arcjets

Arcjets are, like resistojets, electrothermal devices, but the wall temperature limitation of the resistojet is overcome here by depositing power internally, in the form of an electric arc, typically between a concentric upstream rod cathode and a downstream anode that also serves as the supersonic nozzle

(Fig. 2b). The flow structure at the throat is extremely non-uniform, with the arc core at temperatures of 10,000–20,000 K, and the buffer layer near the wall at no more than 2000 K. Because of this there is practically no flow through the arc core, which can be thought of as an effective fluid plug; this reduces the flow, without reducing the pressure integral, and leads to the high specific impulse. On the other hand, some intrinsic loss mechanisms are now introduced.

1) Compared with a uniformly heated stream, the nonuniformity reduces by itself the propulsive efficiency because, as in any thermal propulsion device, maximum thrust for a given power and flow is obtained when the heat is added uniformly across the flow.

2) The power invested in ionizing the arc gas is mostly lost because of the small recombination time available (in addition, in molecular gases, there is a substantial dissociation loss as well).

3) There are near-electrode voltage drops, which mainly constitute a local heat loss to the electrodes.

As with resistojets, the choice of gas is often dictated by considerations unrelated to the thruster itself. Once again, the first practical implementation has been with hydrazine, as the next logical evolutionary step from monopropellant systems. However, arcjets do pose some restrictions (related to arc stability) on the range of stagnation pressures used, which tends to limit blowdown systems to those in which the arcjet portion of the total fuel is relatively small [as in the Lockheed Martin Telstar-4, where most of the hydrazine is used in a bipropellant chemical thruster for geosynchronous Earth orbit (GEO) orbit insertion, the balance going to a 1.8-kW arcjet for NSSK].⁵ Hydrazine arcjets achieve $I_{sp} \approx 500$ –600 s, a significant improvement from resistojets; on the other hand, the efficiency is, for the reasons stated, no higher than 35–40%, which may or may not be critical, depending on the relative importance of fuel vs power savings. Further performance advances will be paced by materials and by thermal design, the goal being to allow the arc to fill most of the throat, without damaging its wall.

Other working gases of potential interest for arcjets are hydrogen and ammonia. Hydrogen has a clear advantage in performance (I_{sp} can easily exceed 1000 s) but suffers from the low storage density and the cryogenic nature of the fuel; it might become practical for missions with continuous thrusting, where the tank could be cooled by the evaporation of the feed. Ammonia yields specific impulses $I_{sp} \approx 800$ –900 s with a liquid fuel, but the propellant system is relatively complex.

The PPU for an arcjet is significantly more complex than that for a resistojet. The discharge voltage is higher than most bus voltages, e.g., 80–120 V, requiring at a minimum dc-dc conversion. In addition, the negative-impedance characteristic of an arc must be handled without the interposition of a dissipative ballast, and special transient modes must be provided for startup. As a consequence the PPU can be several times heavier than the thruster itself (Table 1). The plume is still relatively benign, with divergence angles similar to those of conventional thrusters, and no more than a few percent ionization.

Arcjets occupy an intermediate place in the I_{sp} scale, and will remain a viable option for missions where there is some premium on short-burn duration (lower specific impulse implies higher thrust for a given power), or on thrust over only a portion of the orbit (Sec. V). They will also continue to compete with plasma thrusters in geostationary applications, where they present fewer S/C integration problems (Sec. VI). The Telstar 4 and GE-1 satellite series have featured arcjets (Table 2).

C. Hall Thrusters

The generic configuration of a Hall thruster is shown in Fig. 2c. Gas (usually xenon) is injected through the anode into an annular space and is ionized by counterflowing electrons, which are part of the current injected through an external hollow cathode (the rest neutralizes the ion beam). The ions ac-

Table 1 Typical electric thruster features

Thruster type	Resistojet (N ₂ H ₄)	Resistojet (NH ₃)	N ₂ H ₄ arc	H ₂ arc	NH ₃ arc	Xe Hall	Xe ion	(Pulsed) Teflon PPT	Cs FEFP	MPD (applied field)	MPD (self-field)
Power range, W	500–1500	500	300–2000	5–100 K	500–30 K	300–6000	200–4000	1–200	10 ⁻⁵ –1	1–100 K	200–4000 K
I _{sp} , s (typical)	300	350	500–600	1000	500–800	1600	2800	1000	6000	2000–5000	2000–5000
η (typical)	80%	80%	35%	40%	27–36%	50%	65%	7%	80%	50%	30%
Plume divergence	<20 deg	<20 deg	<20 deg	<20 deg	<20 deg	30–40 deg	<20 deg	—	—	—	—
Peak voltage	28	28	100	200	—	300	900	1000–2000	6000	200	100
Thruster mass, kg/kW	1–2	—	0.7	0.5	0.7	2–3	3–6	120	—	—	—
PPU mass, kg/kW	1	—	2.5	2.5	2–3	6–10	6–10	110 (includes capacitor)	—	—	—
Miscellaneous ^a (per thruster)	1	—	5	5	—	10	10	Small	—	—	—
Tankage fraction	0.05	—	0.05	0.15	—	0.12	0.12	—	—	—	—
Propellant management	Standard blowdown	Regulated	Regulated or low-range blowdown	Regulated or low-range blowdown	—	Regulated	Regulated	—	Cs boiler	—	—
Propellant storage	Stable liquid	Liquid	Stable liquid	Cryogenic H ₂	Stable liquid	Supercritical Xe (ρ ≅ 1.5 g/cm ³)	Supercritical Xe (ρ ≅ 1.5 g/cm ³)	Solid	Solid/liquid	NH ₃ , H ₂ , A	NH ₃ , H ₂ , A
Lifetime, h	500	—	>1000	—	1500	>7000	10,000	>10 ⁷ pulses	—	—	—
S/C interaction concerns	—	—	Thermal radiation	Thermal radiation	—	Wide plume, ion backflow, torque	Ion backflow, nonpropellant effluent	Plume condensation	Cs contamination	—	—
Status	Operational	—	Operational	Lab	Qualified	Operational	Operational	Operational	Development	Lab	Lab/development
Typical mission	NSSK orbit insertion, deorbit	Orbit corrections	NSSK	Orbit transfer (medium ΔV)	NSSK, orbit raising	NSSK orbit raising (medium ΔV)	NSSK orbit transfer (large ΔV)	Small orbit corrections (precision)	Small orbit corrections (precision)	Large ΔV, medium power	Large ΔV, high power
References	2, 3	3, 4	5, 6	7	8, 9	10, 11	12–14	15, 16	17	18	19

^aCable, gimbal, thermal control, structure, propellant feed (power range 0.5–2 kW).

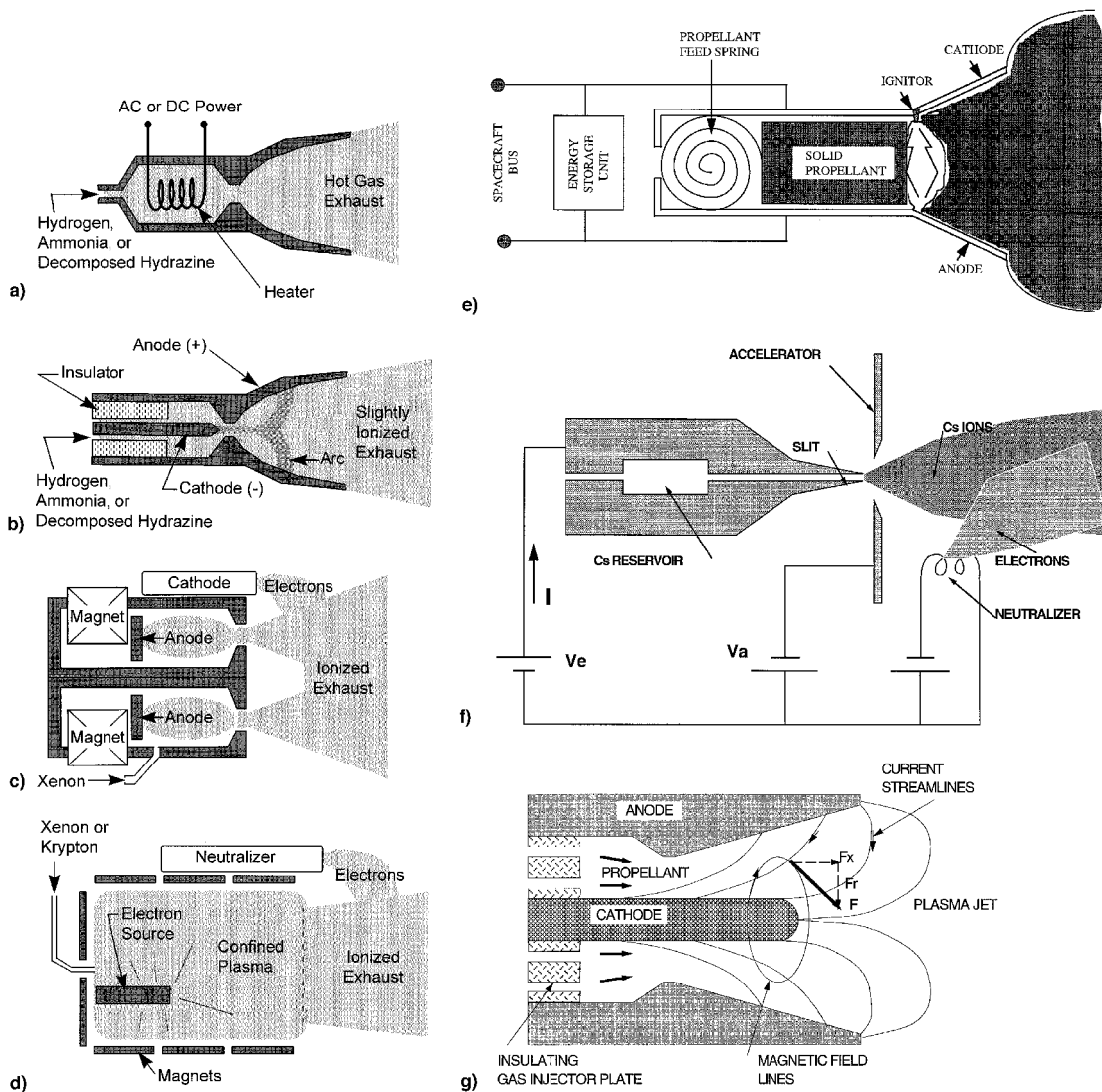


Fig. 2 Operating principles of a) resistojets, b) arcjets, c) Hall thrusters, d) ion engines, e) pulsed plasma thrusters, f) field-effect electrostatic propulsion thrusters, and g) self-field magnetoplasmadynamic thrusters.

celerate under the electrostatic field impressed by the negative cathode, and are only weakly deflected by the imposed radial magnetic field. The electrons, however, are strongly magnetized, and are forced to execute an azimuthal drift (Hall current), while slowly diffusing axially across the field toward the anode (from where the power supply pumps them to the cathode). Thus, Hall thrusters belong, with ion engines, to the class of electrostatic ion accelerators; on the other hand, the thrust is transmitted to the magnetic coils through their interaction with the electron Hall current, justifying the name. The gas density is low enough to ensure near collisionless ion flow, and so a Hall thruster is many times wider than an arcjet of similar power (but still more compact than ion engines).

The plume is highly (sometimes fully) ionized, but there are no dissociation losses, and the ionization loss is somewhat diluted by the higher operating voltage (about 300 V for $I_{sp} \cong 1500$ s). There is $\sim 5\%$ I_{sp} loss as a result of the gas flow in the hollow cathode; otherwise the electrode losses are small. These thrusters achieve efficiencies in the 45–55% range, increasing slowly with voltage (specific impulse). Because most of the flow leaves as ions, the current is controlled by the flow rate; owing to the very low flows involved (a few mg/s), this flow control is a nontrivial task and is accomplished either by thermally varying the gas viscosity in the feed capillaries, or, more recently, by precision electromechanical valves. For a given flow, thrust, specific impulse, and power can be con-

trolled through the voltage. Some additional control can be exerted through the magnetic field, although for simplicity, the magnetic coils tend to be placed in series with the main discharge. The PPU is here even more complex and heavy than for arcjets (see Table 1), as plasma fluctuations have to be accommodated, and the magnet current and flow controls coordinated as well.

In addition to the ceramic-lined stationary plasma thruster (SPT) type, a competing Hall thruster design that offers about twice the thrust density (but very similar performance) is the so-called “thruster with an anode layer” (TAL), in which the walls are metallic, and the channel is shorter and narrower. Flight development and qualification of TAL thrusters is still under way.

Because of their relatively high efficiency at moderately high specific impulses, Hall thrusters are found to be optimal for many applications and, having a substantial orbital pedigree in Russia (see Sec. VII), are now available for many Western missions. These include NSSK applications for several satellite series, as well as plans for deployment and orbit control for some low Earth constellations. In a series of qualification tests to Western standards, the particular SPT type has demonstrated 7000 h of operational life (limited by erosion of the confining ceramic walls), which is sufficient for most of these missions. TAL thrusters have not undergone this kind of life testing, but the fact that the denser part of the plasma

Table 2 Operational flights of electric thrusters

First launch	Vehicle type/ number on-orbit	Thruster type/ number per vehicle	Kilowatts per thruster	Thruster function	Sponsor/builder
Attitude control:					
1964	Zond-2/1	Teflon-pulsed plasma/6	<0.10	Sun pointing	Russia
1987	Kosmos/2	Xenon plasma, SPT-70/6	0.75	Attitude control, orbit ad- justment	Russia/Fakel
Geosynchronous stationkeeping:					
1968	LES-6/1	Teflon-pulsed plasma/4	<0.01	EWSK	USAF/FHC + MIT
1980	INTELSAT-V/13	Hydrazine resistojet/4	0.35	NSSK	Ford/TRW
1982	Kosmos, Luch/13	Xenon plasma, SPT-70/4	0.75	EWSK, reposition	NPO PM/Fakel
1983	Satcom-1R, etc./32	Hydrazine resistojet/2,4	0.60	NSSK	RCA/RRC
1993	Telstar-4, etc./12	Hydrazine arcjet/4	1.8	NSSK	LM/OAC
1994	Gals, Express/5 ^a	Xe plasma, SPT-100/8	1.35	NS and EWSK	NPO PM/Fakel
1994	ETS-6, COMETS	Xenon ion, IES 12 cm/4	0.73	NSSK	NASDA/MELCO
1994	GOMS (Electro)/1	Ammonia resistojet/16	0.45	EWSK, attitude control	Russia/NIIEM
1996	GE-1, etc./9 ^a	Hydrazine arcjet/4	2.0	NSSK	LM/OAC
1997	PAS-5, Galaxy 8-i/2	Xenon ion, XIPS-13/4	0.44	NSSK, attitude control	Hughes
1998 ^b	Galaxy-10/1	Xenon ion, XIPS-25/4	4.5	NSSK, attitude control	Hughes
2000 ^b	ARTEMIS/1	Xe ion, UK-10, RIT-10/4	0.60	NSSK	ESA/RAE + MBB
2000 ^b	Stentor/1	Xe plasma, PPS-1350/4	1.5	NSSK	CNES/SEP + Fakel
2000 ^b	DRTS/2	Hydrazine arcjet/4	1.8	NSSK	MELCO/NASDA
Other orbit adjustments:					
1965	Vela/2	Nitrogen resistojet/1	0.09	Phase adjustment	USAF/TRW
1965	U.S. Navy satellite/5	Ammonia resistojet/2?	0.03	Orbit adjustment	U.S. Navy/GE
1967	Advanced Vela/6	Nitrogen resistojet/2	0.03	Phase and spin adjustment	USAF/TRW
1971	U.S. Navy satellite/4	Ammonia resistojet/2	0.01	Orbit adjustment	U.S. Navy/AVCO
1974	Meteor-18, etc./4	Xenon plasma, SPT-60/2	0.45	Orbit adjustment	Russia/Fakel
1976	TIP/2, NOVA/3	Teflon-pulsed plasma/2	0.03	Drag compensated	U.S. Navy/RCA + APL
1981	Meteor 3-1, etc./10	Ammonia resistojet/4	0.45	Orbit adjustment	Russia/NIIEM
1988	Gstar-3/1	Hydrazine resistojet/2,4	0.60	Orbit transfer	RCA/RRC
1997	Iridium/72 ^a	Hydrazine resistojet/1	0.50	Orbit adjustment	Iridium/OAC
1998 ^b	AMSAT P3D/1	Ammonia arcjet/1	0.70	Orbit adjustment	AMSAT/IRS
1998 ^b	New Millenium, DS-1/1	Xenon ion, 30 cm/1	2.4	Orbit transfer	NASA/Hughes
2000 ^b	MightSat II.1/1	Teflon-pulsed plasma/1	0.10	Orbit transfer	USAF/Primex

^aTotal expected by 1998. ^bPlanned launch date.

in these engines is formed outside the annular channel may favor longer life. Some of the remaining concerns are as follows.

1) A wide plume dispersion angle, which forces alignment at angles of 30–40 deg to solar arrays or other sensitive areas.

2) Under some operating conditions (and mostly in SPTs), deep current fluctuations at a few tens of kHz, together with a variety of higher frequency (but less deep) plasma fluctuations; this may pose communications interference problems if the plume intersects the antenna pattern.

3) A small torque about the axis because of magnetic forces on the ions; this amounts to about 2% of the product of thrust and diameter, and is easily countered by pair arrangements or small auxiliary thrusting.

Hall thrusters have flown (Table 2) on the Kosmos, Luch, Gals/Express, Meteor 18, and Meteor 3-1 satellites in addition to several test S/C.

D. Ion Engines

In gridded electrostatic ion accelerators (Fig. 2d), ions are produced in a separate, magnetically confined ionization chamber, usually by an auxiliary dc discharge, although one can also use radio-frequency power [as in the European radio-frequency for thrusters (RITs)], or tuned electron cyclotron resonance (ECR ionizer). One side of this chamber is covered by a double-grid structure, with spacing of the order of $\frac{1}{2}$ –1 mm, across which the ion acceleration voltage is applied. Ions that wander into the thin sheath covering the inner (screen) grid fall through and are extracted and accelerated, the ion optics geometry being designed to avoid impact on the accelerating outer grid. Electrons are absent in the grid gap, which limits the extracted current below that level for which repulsion by ions in that gap would keep new ions from entering (space charge limit). The electric field at the inner surface of the accel grid is strong, and its pull on the grid transmits the thrust to the structure. Electrons are extracted from the ioni-

zation chamber through an anode (so that at least one dc electrode is present, even in radio frequency devices), and pumped by the power supply to an external hollow cathode/neutralizer held slightly above the potential of the accel grid. Unlike Hall thrusters, the magnetic field in ion engines plays a secondary role, limited to delaying the loss of primary ionizing electrons.

Because of the space charge limitation, ion thrusters are bulkier for the same thrust than Hall thrusters, in which electrons neutralize the plasma everywhere. Because they optimize at high specific impulse, they provide less thrust per unit power. They also have a more complex set of power supplies and controls, with PPU masses of the order of 7 kg/kW (Table 1). On the other hand, they offer substantially better control of the plasma location and operating parameters, which translates into 1) longer life, with 10,000 h demonstrated; and 2) better efficiency, at least at specific impulses above ≈ 2500 s (but Hall thrusters may evolve in that direction and compete); and 3) less beam divergence, but still requiring beam canting of the order of 30 deg away from solar arrays. One further advantage of ion engines is their technological maturity; development challenges tend to be limited to life extensions through better materials, and simpler and lighter PPUs.

Ion engines are the thrusters of choice for deep missions, requiring high ΔV and tolerating long thrusting times, such as interplanetary orbit transfers. The high specific impulse advantage may be partially lost in NSSK applications if low available power forces nearly continuous thruster operation, including inefficient orbital locations (Sec. V), but they are still quite competitive for this application. Ion engines have flown operationally on the Japanese ETS-6 and COMETS satellite, plus PAS-5 and Galaxy 8-1 (from Hughes Space and Communications Co.), and additional flights are forthcoming.

E. Pulsed Plasma Thrusters

Pulsed plasma thrusters (PPTs) differ from all other concepts discussed here in two fundamental ways: they operate in short

($\approx 10\text{-}\mu\text{s}$) pulses and, in their most developed form, they use a solid propellant (Teflon[®]). Figure 2e shows the general arrangement; the only moving part is the spring pushing the solid propellant bar. A capacitor is charged from the primary power supply and applies 1–2 kV across the exposed Teflon face; a spark plug initiates the discharge, which may be shaped by additional pulse-forming circuitry, and the combination of thermal flux, particle bombardment, and surface reactions, depolymerizes, evaporates, and mostly ionizes a small amount of material ($\approx 1.5\ \mu\text{g/J}$). The instantaneous current is in the tens of kA, and the self-induced magnetic field is high enough to create a magnetic pressure comparable to the gas kinetic pressure in the thin ionized layer; the combination of both pressure gradients accelerates the slug of gas to speeds up to the vicinity of the “critical Alfvén velocity,” at which the kinetic energy equals the ionization energy.¹⁶ This usually translates to specific impulses of 1000–1500 s, or higher at very high power.

An appealing aspect of PPT technology is the integration of a nontoxic propellant feed system with the thruster in a single compact unit. A second positive aspect is the intrinsic flexibility that permits a given device to operate over a very wide range of mean power or thrust by simply varying the repetition rate. This lends itself well to precision orbital or attitude-control tasks, and PPTs have indeed been in use for such applications since the late 1960s, starting with the LES-6 satellite, and continuing with the U.S. Navy’s NOVA constellation. To counter these advantages, the efficiency has so far been no higher than 8–13%, the thrusters have been fairly massive (eight times the propellant mass in the case of the well-developed LES 8/9 thruster), and the arrangements required for feeding large propellant masses for deep missions appear awkward. Both NASA and the AF have launched technology programs designed to remedy some of these problems.¹⁵ The efficiency can be raised by pulse tailoring, nozzle recovery of more of the thermal energy, and operation at higher instantaneous power. The mass can probably be cut in half by redesign and improvements in capacitor and electronic technologies. Some recent work at Princeton University suggests the possibility of operating with a valve-less gas feed, which would simplify the fuel logistics.

In the short term, PPT remains an excellent option for relatively light propulsion applications, if reliability and precision control are important criteria. As the technology progresses, there is the future potential for other, more demanding propulsive tasks as well. Aside from the early Zond-2 and LES applications, TIP and NOVA spacecraft have featured PPTs and other applications will soon follow.

F. Field-Effect Electrostatic Propulsion

Field-effect electrostatic propulsion (FEEP) is another unique technology for very high specific impulse, low-thrust applications. The physical basis is the ability of strong surface electric fields ($\approx 1\ \text{V}/\text{Å}$) to extract individual ions from a metal lattice, particularly the easily ionizable alkalis. The implementation that has been perfected in Europe uses liquid cesium for this purpose (see Fig. 2f). The high field is created at the tip of a two-dimensional capillary feed channel (depth $\approx 1\ \mu\text{m}$) with sharp lips, by an extractor electrode placed 0.5–1 mm in front of it. Neutralization is done by a field-effect microtip array, which can emit $\approx 1\ \text{mA}/\text{mm}^2$ with a bias of the order of 100 V. This would be an excessive voltage for traditional electrostatic thrusters, but FEEP requires a primary voltage in excess of about 6000 V to initiate ion extraction, making the relative neutralization loss negligible. At a typical extraction-acceleration voltage of 10 kV, the specific impulse is about 10,000 s, so that, although the efficiency is high, the thrust per unit power is very small (16 $\mu\text{N}/\text{W}$). For most missions, the fuel usage would be so small that the Cs would be incorporated in a recess of the emitter structure. Thrusters with slit widths of a few millimeters to a few centimeters, and a thrust of 1 μN to 5 mN have been developed and tested, but not yet in space.

FEEP is, along with colloidal ion engines, one of the few EP technologies that does not rely on gas-phase ionization. This may prove to be important in the context of micropropulsion because it relaxes the requirement for electron collision mean free paths to shrink with the plasma dimension and, thus, avoids the serious container lifetime issues that the increased fluxes entail. On the other hand, two objections arise in the FEEP case.

1) The very low thrust/power ratio, which limits applicability to either low-thrust precision control or extremely high ΔV missions, beyond foreseeable applications.

2) The use of liquid Cs, with its known potential for chemical attack on many surfaces where it may deposit. Additional development work may be needed to overcome some secondary problems, like the high sensitivity to surface contamination.

G. Colloidal Ion Thrusters

The original impulse for the development of this type of thruster in the 1960s was the need for thrusters that would yield higher thrust density and would be efficient at lower specific impulse than ion engines. The principle is analogous to that in FEEP, except that a nonmetallic liquid is used, and submicron-sized charged droplets are extracted rather than individual ions. Intensive NASA-led efforts at that time were frustrated by the inability to increase the charge/mass ratio of the extracted droplets sufficiently, which forced the use of very high voltages (several tens to hundreds of kV) to reach the desired specific impulse range (around 1000 s). There was also difficulty in obtaining sprays with nearly uniform values of the charge/mass ratio, which led to poor beam focusing. With continued development of the charged spray technology for applications such as printing and paint application, some of these limits have been relaxed. Russian work²⁰ has led to the development of 65% efficient colloidal engines in the 1000-s specific impulse range that operate with voltages of 15–25 kV.

This type of thruster would appear to be a leading contender for micropropulsion applications requiring high ΔV at moderately high thrust/power ratios.

H. Magnetoplasmadynamic Thrusters

As in electrical machinery, higher-power densities are generally achievable in plasmas through magnetic rather than through electrostatic interactions [$B^2/2\mu_0 \gg (\epsilon_0/2)E^2$, for realizable fields]. The self-field magnetoplasmadynamic (MPD) thruster (Fig. 2g) creates an azimuthal B field, and a corresponding magnetic pressure, by passing a strong radial current between concentric electrodes (the same basic principle as in PPT discharges, but with a different geometry). The thrust is proportional to magnetic pressure, hence to I^2 (I being the current), and because the thrust power is $F^2/2m$, the back emf (useful part of the voltage) scales as I^2/m . This means that at low currents ohmic and near-electrode voltage losses will dominate, and the efficiency will be low (although, as with PPTs, some recovery of the ohmically dissipated power may be possible). In practice, MPD thrusters using noble gases have not exceeded 35% efficiency, even at megawatt power levels ($I_{sp} \approx 2000\ \text{s}$). Better efficiencies have been obtained with hydrogen, at much higher specific impulses.

A noteworthy MPD feature is the development at high currents and low flow rates of a strong plasma pinching force, associated with the Hall currents (which in this geometry are axial). The result is an eventual poor connection of the plasma with the outer electrode (anode), preventing the achievement of high enough specific powers and, hence, efficiencies. This difficulty can be overcome by arranging for a fraction of the gas to be fed through the anode, at the cost of additional complexity.

Because of the MPD thruster’s high-power requirements and capabilities, it has been long regarded as a leading candidate for future space missions such as heavy-lift Mars transfer, in

conjunction with a nuclear powerplant. But, aside from the current lack of such powerplants, the high-power character of MPD has also slowed its development because no adequate vacuum pumping capacity has existed for steady-state laboratory operation. Lacking that resource, testing in pulses of about 1 ms duration, long enough to reach quasi-steady flow, but not adequate for most wall interaction studies has been done. At this time, MPD is still an experimental technology, in need of much refinement. A pulsed, self-field MPD thruster was recently space-tested on the Japanese Space Flyer Unit (SFU) spacecraft.¹⁹

A related technology, perhaps more amenable to near-term application, is the so-called "applied field MPD thruster." In this type of thruster, an external solenoid produces a field with meridional lines of force, arranged so as to diverge in nozzle fashion toward the exit. This introduces an azimuthal electron drift current, akin to that in Hall thrusters, although here the collisionality is higher, and the drift does not come near closing on itself. It does, however, serve to create an additional component of thrust ($I_0 B_r$) to supplement that due to the self-induced field pressure, plus the thermal component. Because of this, efficient operation at lower powers is easier to obtain. The combination of several types of effects makes the physics of this thruster more difficult to understand and optimize, and development has lagged. Results with noble gases have been disappointing, but hydrogen (again, at high specific impulses) has indicated over 50% efficiency. Recent work on lithium-fed MPD thrusters has yielded over 40% at only 130 kW, with $I_{sp} \approx 3500$ s. Lithium propellant has another important advantage, in that it drastically reduces erosion to the central cathode, through which it is injected. On the other hand, as noted in connection with FEEP, the use of alkali metals as propellants raises many S/C compatibility issues.

IV. Power Sources for EP

Some simple relationships will illustrate the principal factors affecting the selection and the performance of an EP system. For a mission requiring a velocity increment ΔV in a thrusting time t_r , the mean acceleration is $\Delta V/t_r = F/m$, where F is the thrust and m is the S/C mass; here, F/m is to be understood as a mission average, although in some cases it is actually optimal to maintain this acceleration constant. The power into the thrusters is related to thrust, efficiency (η), and effective jet speed c (related to specific impulse through $c = g_0 I_{sp}$) by $P = Fc/(2\eta)$. Combining these relationships, the required thrusting time is

$$t_r = \frac{c\Delta V}{2\eta(P/m)} \quad (1)$$

This shows the importance of a high value of the specific power P/m to reduce the mission time. It also illustrates the importance of high efficiency for the same purpose, and it indicates that shorter missions are possible with a lower specific impulse (but, of course, using more propellant). As an illustration, EP orbit raising from LEO to GEO requires on the order of a 6000 m/s velocity increment (Sec. V). If this is to be done in six months using a Hall thruster system of $\eta = 0.5$ and $I_{sp} = 1500$ s ($c \approx 15,000$ m/s), Eq. (1) indicates that a specific power $P/m = 5.7$ W/kg is required. This is feasible for a vehicle designed with a propulsion-dedicated solar array, and orbital transfer vehicles of this type have been proposed. Interestingly, this specific power is also not too far above the range of values present for payload use in many modern S/C (Fig. 3). One conclusion is therefore that many missions slightly less ambitious than complete LEO-GEO transfer are now feasible without the need for a dedicated power supply; some of these will be considered in Sec. V.

Although nuclear reactors and solar thermal converters have been considered as future power source technologies for EP, solar photovoltaic cells presently appear to be the only prac-

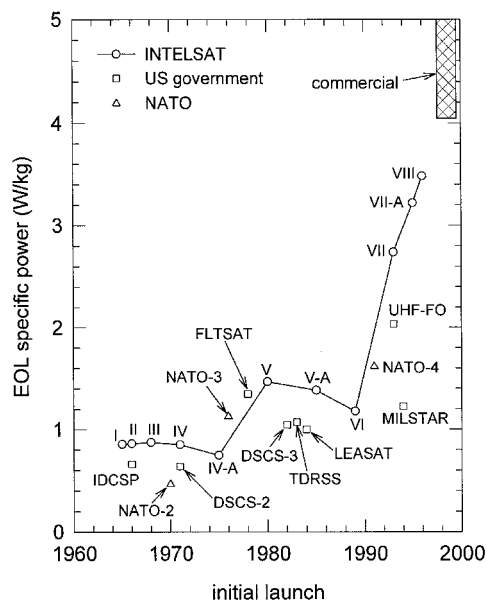


Fig. 3 Spacecraft specific power at end-of-life for geosynchronous satellites.

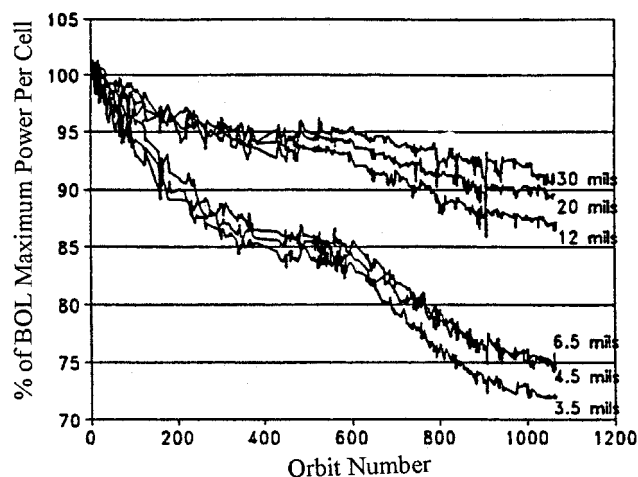


Fig. 4 Output power for GaAs/Ge solar cells measured during the CRRES mission with six different thicknesses of quartz cover glass. Data were recorded during a period of 440 days and normalized to conditions at beginning of life.

tical alternative (with the exception of outer planet missions). Cell technology continues to advance along several fronts.²¹ Arrays using the standard silicon cells deliver 140 W/m², and 40 W/array kg, at a cost of \$1000–1500/W. Gallium arsenide cells are now fully qualified for space use, produce 220 W/m², are more resistant to radiation, and can operate at a higher temperature. Indium phosphide cells have performance levels similar to gallium arsenide, and are even more tolerant to radiation, but their cost is much higher. Combining several semiconductors into a multijunction cell yields 300 W/m², as in the Lewis satellite for NASA.

One cost-efficient and low-weight technique for the use of advanced GaAs or InP cells, particularly for high radiation environments, is to incorporate concentrators with concentration ratios of 10–200. This requires better pointing, with the angular tolerance typically decreasing from ± 18 deg (flat panel) to ± 3 deg). Designs based on linear parabolic Fresnel refractors²² or on foldable Cassegrainian elements made of aluminumized Mylar promise about 100 W/array kg in the next few years. Even higher-power density is projected for flexible blanket arrays,²³ although in this case the radiation resistance is sacrificed because of the thin substrates and cover glasses.

Table 3 Minimum spacecraft specific power to enable NSSK with EP

Thruster	Specific impulse, s	Thrust efficiency	Power processor efficiency	Cant angle, deg	Specific power, W/kg
Xenon ion engine	3000	0.55	0.88	30	≥ 1.70
Xenon Hall thruster	1480	0.43	0.93	40	≥ 1.14
Hydrazine arcjet	520	0.35	0.91	20	≥ 0.41
Hydrazine resistojet	300	0.88	1.00	20	≥ 0.09

EP-driven vehicles spiraling through the Earth radiation belts will be subjected to large radiation doses. This will affect the payload and other electronics, and the solar arrays.²⁴ Two recent missions, CRRES²⁵ and PASP Plus,²⁶ have provided data on the effects on arrays. CRRES operated for 14 months in a highly elliptic orbit (348 km \times 33,582 km, $i = 18.2$ deg). Figure 4 shows the degradation of the CRRES tested cells for several cover glass thicknesses. Following a sharp initial loss the power was nearly stabilized, but the loss rate resumed after a large solar flare at orbit 587. A cover glass thickness of 12 mil appears to be a good compromise between protection and additional weight. On the other hand, concentrators will allow a much thicker cover (30 mil), so that the degradation for a 180-day LEO-GEO transfer need not exceed 4–6%. PASP Plus has shown that concentrator designs can operate at higher bias voltages without arcing, a fact that can be very beneficial for EP, by reducing or eliminating the need for a voltage-raising PPU.

Many EP missions include periods when the spacecraft is in the Earth's shadow, and batteries must be used for the primary payload. A key design objective for many cases is to be able to operate the electric thrusters to satisfy the propulsive requirements without having to increase the battery capacity. A geosynchronous satellite experiences about 90 eclipses per year, centered about the two equinoxes, and lasting up to 1.2 h, and low orbits undergo about 6000 eclipses per year, lasting 35–40 min each. Recharging batteries typically uses 12% of the array output for a GEO satellite, but 25–40% for a LEO satellite.

V. Typical EP Missions

Although other applications are possible, only three mission categories are illustrated: stationkeeping in GEO orbit, orbit raising or lowering, and orbital repositioning.

A. NSSK

The dominant propulsive requirement for a geosynchronous satellite is usually the so-called NSSK function. The orbit of the moon is near the ecliptic plane, and so around midsummer and midwinter, the gravity gradient (tidal effect) of the sun and moon have components directed out of the equatorial plane toward the ecliptic each time the S/C is roughly in line with the Earth and one of these bodies. Over the year, this averages to a torque pointed along the equinox line, and results in a secular gyroscopic rotation of the orbital plane about an axis perpendicular to it, at a rate of 0.75–0.95 deg/year (depending on the current phase in the 18.6-year precession of the Moon's orbital axis). If left uncompensated, this would result in an initially geostationary satellite describing a growing elongated North–South figure-8, as seen from Earth. Most GEO satellites require positional accuracy to 0.05–0.1 deg, which necessitates either occasional or near-continuous propulsive corrections amounting to between 41 and 51 m/s/year. Given the 12–15 years of design life of many of these satellites, this is not an unsubstantial ΔV , and the fuel-saving nature of EP is beneficial here.

From the nature of the disturbances, it can be seen that the NSSK propulsive corrections should be 1) directed out of the orbital plane, in the N–S direction, and 2) concentrated near the solstitial line, to be in counterphase with the tidal perturbations. One interesting consequence is that, even in the near-

equinoctial periods in which eclipses occur, the propulsive maneuvers will take place around 6 a.m. and 6 p.m. and will be in sunlight. Therefore, provided the array can recharge batteries in 3–5 h after the eclipse's end, EP can be used for NSSK throughout the year with two firings per day (alternatively, if only one firing per day is used, the charging time can be relaxed). Assuming that at array end-of-life the only power available for thrusting is from the batteries, which are dimensioned to supply the basic load during the 1.2 h of the longest eclipse, the maximum thrusting energy is the basic power, times 1.2 h. Thus, regardless of how the thrusting is actually distributed over time, we can use Eq. (1), with $\Delta t = 1.2 \times 365$ h/year and, on average, $\Delta V = 46$ m/s/year to estimate the required S/C specific power. The efficiency η should include an allowance for the fact that thrusting off-solstice is not fully effective [for a firing arc β this is expressed by a factor $\eta_{\text{NSSK}} = 2 \sin(\beta/2)/\beta$], a cosine factor for the canting angle of the plume away from the N–S line (where the array is) and also a battery charge-discharge efficiency. The results for a number of thruster types are shown in Table 3; by comparison with Fig. 3, it can be seen that many current S/C can indeed provide the required power. Over 40 S/C currently use or have used resistojets, 20 use arcjets, five use Hall thrusters, and five use ion thrusters for NSSK.

In addition to the NSSK function, GEO satellites normally require also some east–west corrections (EWSK) because of the slightly elliptical shape of the Equator, which produces stable points at 74°E and 104°W and unstable points at 162°E and 12°W. The maximum required ΔV for this purpose is 1.9 m/s/year. This correction can be applied by the same thrusters as the NSSK correction, if they are mounted with some cant angle component in the EW direction.

B. Orbit Raising

Orbit raising may be required in a variety of contexts: drag compensation, deployment to high LEO orbits from low delivery orbits, total or partial LEO-GEO transfers, interplanetary transfers, LEO altitude changes to allow Earth oblateness to rotate the line of nodes (for constellation deployment), and, by extension, deorbiting of spacecraft at the end of life.

In these cases, if plane change is not involved, the thrust line is mainly along the flight path. For initially circular orbiting, the basic gravity-centrifugal force balance is nearly preserved, and it can be shown that the required ΔV under low thrust is approximately equal to the magnitude of the orbital velocity change, at least until the escape velocity is approached. This is also true for impulsive thrusting if the initial and final radii are within a few percent of each other, but for larger differences, impulsive Hohmann transfers can require significantly less ΔV . For example, raising a 300-km circular orbit to a 1300-km altitude requires almost exactly the same ΔV either way (521 m/s), but a coplanar LEO-GEO transfer (from a 300-km orbit) requires $2429 + 1468 = 3897$ m/s impulsively, compared with 4658 m/s with continuous low thrust. The difference is because the impulsive maneuver is able to apply the largest partial ΔV at the higher initial speed, so that more energy is imparted for the same thrust.

Incidentally, this advantage of impulsive thrust is most dramatic for highly elliptic initial orbits, such as geosynchronous transfer orbit (GTO), where even a small perigee ΔV can result in Earth escape, but continuous low thrust spread over the orbit

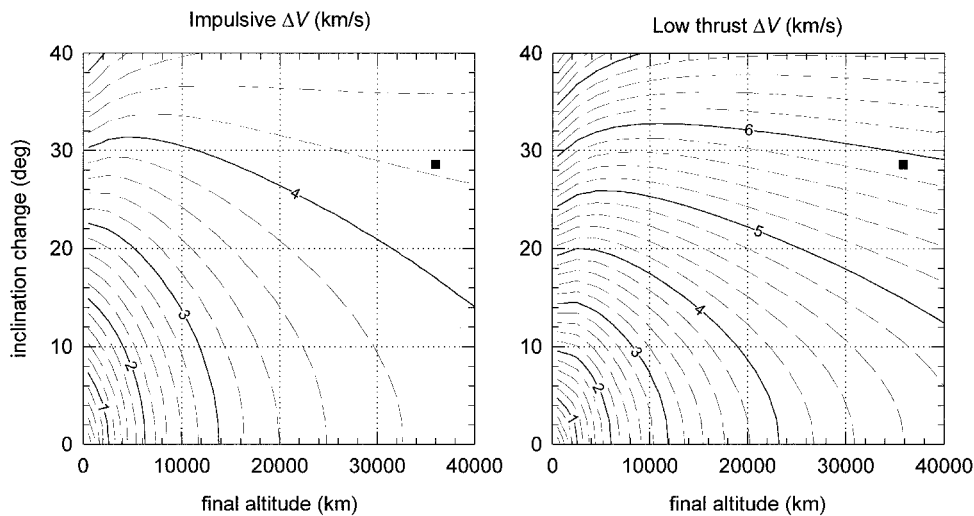


Fig. 5 Contour maps of ΔV for altitude and inclination changes using impulsive and low-thrust maneuvers. The initial altitude is 400 km. Square symbols indicate a LEO-to-GEO transfer from the Cape Canaveral launch site.

is inefficient and requires a much higher ΔV to escape. A partial remedy in these cases is to restrict operation of the low-thrust engines to a fraction of the orbit, concentrated about perigee. This reduces fuel consumption at the cost of a longer mission time, and may not be acceptable in the GTO case because of the increased radiation dose.

Some orbit-raising maneuvers, notably LEO (28.5 deg)-GEO, require a simultaneous plane change. Once again, high thrust has the advantage of allowing the plane change to be performed mainly at apogee, where speed is minimum; this is in addition to the ability to apply thrust exactly at the intended line of orbital plane rotation, as we saw in the NSSK case. For low thrust, optimization studies provide steering laws consisting generally of adding a component of out-of-plane thrust which reverses direction once per orbit (at 90 deg to the line of nodes), and whose amplitude increases as the orbit radius increases.²⁷ Figure 5 shows computed ΔV values for combined altitude and inclination changes; for the case of LEO (28.5 deg)-GEO, the high-thrust ΔV is 4220 m/s, whereas the optimized low-thrust value is 5900 m/s.

C. Orbit Phase Changes

LEO constellations will need rephasing maneuvers to maintain full coverage as satellites fail and are replenished. GEO satellites are occasionally shifted in longitude to serve a new area or provide backup for a degraded or failed satellite. For a negative phase change, the general strategy is to transfer to a higher (slower) orbit, drift in this orbit for some time, and return to the original orbit such as to insert at the predetermined new phase. The opposite applies to a forward phase shift, although there may then be altitude limitations for the lower drift orbit.

If high thrust is used for this purpose, the orbital changes are normal two-impulse Hohmann transfers, requiring approximately one-half orbit each. If the basic orbit has a period T_1 and an orbital velocity V_1 , it can be shown that, to first order, the total ΔV required to accomplish the rephasing in a time t_m is given by

$$\frac{\Delta V}{V_1} = \frac{|\Delta\vartheta|}{3\pi[(t_m/T_1) - \frac{1}{2}]} \quad (2)$$

and that the same expression also gives the fraction $\Delta R/R_1$, where ΔR is the magnitude of the altitude change to the drift orbit.

If rephasing is done using EP, each transfer is a spiral climb or descent, lasting a time, say, t_w , during which the angular velocity is intermediate between those of the original and drift orbits. Depending on available power and allocated mission

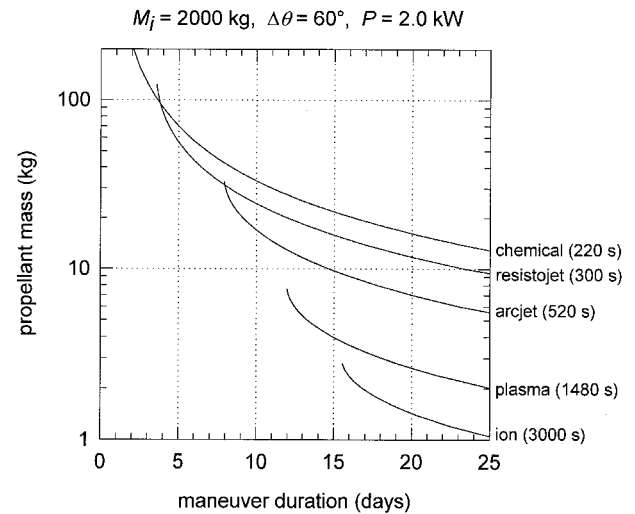


Fig. 6 Propellant mass vs maneuver duration for a 60-deg longitude shift at GEO with a 2000-kg satellite. Thrusters use 2.0 kW and are assumed to be pointed east and west, i.e., no loss because of canting.

time t_m there may or may not be a drift time t_{drift} , and, of course, $t_m = t_{\text{drift}} + 2t_w$. Clearly, reducing the drift time will result in a higher fuel consumption for a given total time and phase angle, because more time is then spent at intermediate drift rates, and a higher final orbit must be chosen to compensate. The resultant expression is now

$$\frac{\Delta V}{V_1} = \frac{\Delta R}{R_1} = 2 \frac{|\Delta\vartheta|}{3\pi} \frac{T_1}{t_m + t_{\text{drift}}} \quad (3)$$

and the required power is

$$\frac{P}{M} = \frac{2c}{3\eta} \frac{R\Delta\vartheta}{t_m^2 - t_{\text{drift}}^2} \quad (4)$$

If no drift is allowed, Eq. (3) indicates nearly twice as much ΔV as for the impulsive case [Eq. (2)]. On the other hand, both methods give similar ΔV if a drift time much longer than the transfer time is allowed. From Eq. (4), allowing a drift time small compared to t_m adds little to the required power, and may be a good option.

Despite the probable disadvantage in ΔV , EP can usually save propellant in these missions, because of the higher spe-

cific impulse. Figure 6 shows typical results for a GEO re-phasing mission.

VI. Spacecraft Interactions

As EP has reached practical applications, many potential interactions with the rest of the S/C have received research attention. This is still a very active area of work and results continue to accumulate, although some of the operational aspects remain in the proprietary domain. Reference 28 provides a review of many of these issues. We summarize several of the salient points regarding plume, thermal, and electromagnetic field effects.

A. Plume Effects

No contamination problems have been reported from operational arcjets. As noted, the arcjet plume is relatively narrow and benign, with ionization falling below 1% near the exit plane. One concern is the potential deposition of some of the metal eroded from the electrodes (3×10^{-5} – 10^{-3} $\mu\text{g}/\text{C}$), although much of it appears to deposit on the nozzle walls, and no external deposition has been noted so far. The plume issue is more important in Hall thrusters. Typically, the plasma density falls by 1/e at about 22 deg from the centerline, and by 1/10 at 45 deg. The composition is about 80–85% single ions, 5–10% neutrals, and 10–15% double ions, and the plasma density (for an SPT-type thruster) is of the order of 2×10^{17} m^{-3} one diameter downstream from the exit (2–3 times higher in TAL thrusters). Because of the relatively high ion density and the disparity between ion and neutral velocities, the rate of production of slow ions via charge exchange (CEX) collisions is high, resulting in a CEX current of the order of 0.1–0.2% of the beam current, mainly in the first one or two diameters from the exit. These slow CEX ions are easily expelled radially from the beam, which is at 5–20 V higher potential than the surroundings. A numerical study²⁹ finds that, because of the self-consistent ambipolar fields set up in the CEX “cloud,” there is also some ion backflow beyond 90 deg from the axis. These ions are not directly attracted to spacecraft negative surfaces if the sheath is thin (LEO operation), but do acquire the sheath energy if they reach its edge, and can produce some sputtering of, for example, the negative end of a solar array. Providing a thruster shield, and placing the thruster far from such negative regions appear to be effective countermeasures. It must be borne in mind in this context that the presence of the plasma plume itself will effectively “ground” the S/C to the ambient potential, even in GEO orbits.

In addition to plasma interactions, the Hall thruster plume may also deposit material sputtered from the thruster walls (typically boron, plus magnet iron toward the end of life). In life tests, the sputtered mass flow amounted to about 1% of the propellant flow initially, decaying to about 0.1% after 4000 h. Some uncertainty remains as to the distribution of this non-propellant efflux (NPE) because of the superposition of tank-

sputtered material, but through the use of collimators to isolate the engine-born NPE, Ref. 30 found them to deposit preferentially between 70 and 85 deg from the centerline, with surfaces closer to the axis being cleaned by beam erosion.

The plasma plume issues are similar in ion engines, and, in fact, more data exist in this case because of the earlier development. The plasma density near the exit plane is about one order of magnitude lower, e.g., 2×10^{16} m^{-3} , than in a Hall thruster, but the neutral density may be higher, e.g., 5×10^{17} m^{-3} , with the result that the net CEX current production is not much lower. CEX events in the acceleration gap may result in high-energy ions flying off at large angles to the centerline. This effect is, however, poorly documented at this time. The plume CEX ions are here less energetic (2–5 eV), but, an additional CEX population can be created by ion-neutral collisions near the accel grid, and these ions can strike the grid with high energy and cause erosion. Deposition of this sputtered engine material can be a problem in ion engines as well, but again, judicious placement and shielding are effective protective measures.

For NSSK applications in GEO satellites, whose solar arrays extend from the north and south faces of the S/C, a conflict arises in that this is also the desired orientation of the thruster plumes. This has forced designs in which the thrusters are canted at angles of as much as 40 deg (Hall) or 30 deg (ion) to the NS line, with a consequent loss of effective specific impulse.

Much less is known about plume effects in other types of electric thrusters. Concern has been expressed about the potential deposition of carbon or carbonaceous material from PPT plumes, but a preliminary experimental study (200,000 pulses) showed no backflow, and only minor effects beyond 60 deg from the axis.³¹ Similar concerns arise in connection with FEEP thrusters, although the volatility of Cs may be an attenuating factor.

B. Thermal Effects

The inefficiencies in the thrusters or in their power processors create thermal loads that may impact S/C design. For applications where the thrusters operate from the basic payload power supply, they do not increase the total power, but even here, they may indeed increase the heat load (depending on what fraction of the payload power is dissipated), and the distribution of heat is also altered. In GEO satellites, for example, a radiator is provided (normally on the NS faces) for the thruster PPU, separate from the payload radiator, so as not to interfere with the payload thermal balance during a firing.

Heat from the thruster itself can be disposed of by direct radiation to space, or in some future advanced arcjets, by regeneration to the propellant. But a fraction may return to the S/C, either by radiation from the body or by the plume, by conduction through the thruster mount, or by plume impingement. Typical power balances for several stationkeeping types of thruster are shown in Table 4.

Table 4 Estimated power balance for stationkeeping thrusters

	Hydrazine Resistojet		Hydrazine arcjet		Xenon Hall thruster		Xenon ion engine	
	Watts	Percent	Watts	Percent	Watts	Percent	Watts	Percent
Input power:								
Electrical (bus voltage)	800	75	1800	96	1450	100	500	100
Chemical	260	25	70	4	0	0	0	0
Total	1060	100	1870	100	1450	100	500	100
Output power:								
Thrust ($\frac{1}{2} F_{\text{sg}} I_{\text{sp}}$)	710	67	570	30	580	40	240	48
Thruster (radiated)	240	23	600	32	250	17	110	22
Thruster (conducted)	<10	<1	<10	<1	<10	<1	<5	<1
Electronics (conducted)	0 ^a	0 ^a	160	9	100	7	60	12
Plume loss ^b	110	10	540	29	520	36	90	18

^aResistojet operates at bus voltage. Surge current limiter dissipates ≤ 90 W per thruster during brief warm-up period.

^bIncludes divergence, ionization, and frozen losses.

Table 5 Experimental flights of electric thrusters

Launch	Experiment/ platform	Thruster type/ number per vehicle	Kilowatts per thruster	Primary data	Sponsor/builder
Subsystems tests:					
1962-64	Scout (3 suborbital)	Cesium ion/1	0.8	Thruster operations	USAF/EOS
1964	SERT-I (suborbital)	Hg ion/1, CS ion/1	1.6	Thruster operations	NASA
1965	SNAPSHOT	Cesium ion/1	<0.5?	Thruster operations	USAF/EOS
1967	ATS-2, -3	Ammonia resistojet/2	<0.01	Thruster operations	NASA/AVCO
1968-69	ATS-4, -5	Ammonia resistojet, Cs ion/4	<0.03	Thruster operations	NASA/AVCO + EOS
1971	Sol Rad-10	Hydrazine resistojet/1	<0.01?	Thruster operations	U.S. Navy/AVCO
1971	Meteor-10	Xe plasma/2; Hg ion/1	0.45	Thruster operations	Russia/Fakel
1977	K-9M-58 (suborbital)	Helium MPD arcjet/1	0.02?	Thruster operations	ISAS
1980	MS-T4 Tansei-4	Ammonia MPD arcjet/2	0.02	Thruster operations	ISAS
1981	MDT-2A (suborbital)	Teflon-pulsed plasma/2	<0.01	Thruster operations	China
1982	ETS-3	Mercury ion, 5 cm/2	0.09	Thruster operations	NASDA/MELCO
1992	RITA/EURECA-1	Xenon ion, RIT-10/1	0.44	Thruster operations	ESA/MBB
1998 ^a	RHETT-2/EPDM	Xe plasma, TAL D55/1	1.5	Thruster operations	BMDO/TsNIIMash
1999 ^a	T-160/Express	Xe plasma, T-160/1	4.5	Thruster operations	BMDO/KeRC
Plume and environmental studies:					
1970	SERT-II	Mercury ion, 15 cm/2	0.84	Plasma and contamination	NASA
1974	ATS-6	Cesium ion/2	0.14	Charge control	NASA/EOS
1975	Kosmos-728	Potassium MPD/1	3.00	Plasma effect	Russia
1981	ETS-4	Teflon-pulsed plasma/4	0.01	EMI effect	NASDA/ETL
1983	SEPAC/Spacelab-1	Argon MPD/1	0.13	Charge control	ISAS
1980s ^b	IAPS/P80-1	Mercury ion, 8 cm/2	0.13	Plasma and contamination	NASA/Hughes
1987	Shadow/Kosmos	Cesium arcjet/2	1.5	Plasma effect	TsNIIMash
1995	EPEX/SFU-1	Hydrazine MPD arcjet/1	0.43	EMI and plume	ISAS/IHI + MELCO
1998	ESEX/ARGOS	Ammonia arcjet/1	26.0	EMI and contamination	USAF/TRW + Primex

^aPlanned launch date. ^bSpacecraft built but never launched.

In resistojets, the PPU loss is small during steady-state firing because only a surge limiter is involved. These devices are well insulated to retain as much heat in the body as possible.

In contrast, arcjets operate so hot (nozzle outside temperatures of 1200–1700 K) that the design emphasizes direct radiative cooling, using coatings to increase the emissivity to near unity. A shadow shield or a thermal blanket is necessary to protect the S/C because calculation shows that surfaces at 20 cm from a 1.8-kW arcjet receive about 1 sun equivalent radiative flux from it. The thruster must also be thermally isolated by mounting it at the end of a long, thin Mo-Re tubular standoff; this results in the low conductive heat loss shown in Table 4. Surfaces near the plume may also be heated by direct impingement; this component dominates over radiation for angles less than about 80 deg from the axis. Radiation from the plume itself has been shown to be insignificant.

Thermal isolation problems are less prominent for ion or Hall thrusters, which have larger radiating areas and operate at lower temperatures.

C. Field Efflux

Electromagnetic interaction (EMI) can take the form of either the plasma noise, caused by a variety of instabilities and fluctuations, or from radio interference caused by scattering or phase distortion by the ionized plume. A survey by Sovey et al.³² found no radio-frequency interference from the early experiences of the SERT II and ATS-6 ion-propelled spacecraft. In more recent tests of a 1.4-kW arcjet,³³ EMI emissions were found to be below MIL-SPEC limits, except below 40 MHz.

Hall thrusters present potentially a unique problem because of the occurrence in some regimes of deep (up to 100%) current oscillations, at frequencies of 20–60 kHz, accompanied by a number of other, higher-frequency oscillations. Dickens et al.³⁴ measured phase shifts of 5–20 deg when passing a 6.2-GHz radio signal through the plume of SPT and TAL thrusters (particularly the former). No serious effects were reported, however, from the earlier Russian flights using this type of thruster.

VII. Flight Experience with EP

Tables 2 and 5 summarize the history of EP space flight for operational (Table 2) and experimental (Table 5) purposes. A

more detailed account of this history can be found in Ref. 35. There has been a more or less steady rate of 4–7 experimental flights worldwide per decade, starting in the mid-1960s. But, more significantly, the number of operational flights has gone from 4 in the 1960s to 11 in the 1970s, 53 in the 1980s, and on the order of 100 in the 1990s (through 1997). This makes it clear that EP is in the midst of a rapid transition from experimental to applied technology, different thruster families being at different points along their maturation curves. It also seems clear that a permanent application niche has been established for a variety of auxiliary propulsion applications.

VIII. Conclusions

This paper has provided a condensed overview of the electric propulsion field, at a time when it is undergoing a very rapid transition from the laboratory to actual flight application. Inevitably, this means that many of the points made here will become obsolete in a short time, and that important emerging technologies may have been missed, for which the authors apologize in advance. Considerably more detail on most of the topics covered can be found in the companion papers in this same issue of the *Journal of Propulsion and Power*. The overall impression is one of substantial maturation in several important areas, compared to only a few years ago, as shown, for example, in the attention being paid to system integration issues and to the nonthruster parts of the propulsion system. At the same time, it also appears that important performance improvements are still possible in most cases, and that the area will remain a vital research field for the foreseeable future.

Acknowledgment

The authors acknowledge the valuable help of S. W. Janson, of The Aerospace Corporation, on several of the topics covered in this paper.

References

- Filliben, J. D., "Electric Thruster Systems," Chemical Propulsion Information Agency Rept. CPTR 97-65, June 1997.
- Dressler, G. A., Morningstar, R. E., Sackheim, R. L., Fritz, D. E., and Kelso, R., "Flight Qualification of the Augmented Hydrazine Thruster," AIAA Paper 81-1410, July 1981.

- ³Miyake, C. I., and McKeivitt, F. X., "Performance Characterization Tests of a 1 kW Resistoject Using Hydrogen, Nitrogen and Ammonia as Propellants," AIAA Paper 85-1159, July 1985.
- ⁴Koroteev, A. S., and Rylov, Y. P., "Development and Application of Electrothermal Thrusters on Russian Spacecraft," 45th Congress of the International Astronautical Federation, Paper 94-S.3.424, Jerusalem, Israel, Oct. 1994.
- ⁵Smith, W. W., Smith, R. D., Yano, S. E., Davies, K., and Lichtin, D., "Low Power Hydrazine Arcjet Flight Qualification," *Proceedings of the 22 International EP Conference* (Viareggio, Italy), Centrospazio, Pisa, Italy, 1991 (IEPC Paper 91-148).
- ⁶Birkan, M. A., and Myers, R. M., "Introduction to Arcjets and Arc Heaters: Research Status and Needs Special Section," *Journal of Propulsion and Power*, Vol. 12, No. 6, 1996, p. 1010.
- ⁷Auweter-Kurtz, M., Gölz, T., Habiger, H., Hammer, F., Kurtz, H., Riehle, M., and Sleziona, C., "High-Power Hydrogen Arcjet Thrusters," *Journal of Propulsion and Power*, Vol. 14, No. 5, 1998, pp. 764-773.
- ⁸Polk, J. E., and Goodfellow, K. D., "Results of a 1462 Hour Ammonia Arcjet Endurance Test," AIAA Paper 92-3833, July 1992.
- ⁹Zube, D. M., Messerschmid, E. W., and Dittmann, A., "Project ATOS: Ammonia Arcjet Lifetime Qualification and System Components Test," AIAA Paper 95-2508, July 1995.
- ¹⁰Kim, V., "Main Physical Features and Processes Determining the Performance of Stationary Plasma Thrusters," *Journal of Propulsion and Power*, Vol. 14, No. 5, 1998, pp. 736-743.
- ¹¹Sankovic, J. M., Haag, T. W., and Manzella, D. H., "Operating Characteristics of the Russian D-55 Thruster with Anode Layer," AIAA Paper 94-3011, June 1994; also NASA TM 106610, June 1994.
- ¹²Kerslake, W. R., and Ignaczak, L. R., "Development and Flight History of SERT II Spacecraft," AIAA Paper 92-3516, July 1992.
- ¹³Beattie, J. R., Matossian, J. N., and Robson, R. R., "Status of Xenon Ion Propulsion Technology," *Journal of Propulsion and Power*, Vol. 6, No. 2, 1990, pp. 145-150.
- ¹⁴Sovey, J., et al., "Development of an Ion Thruster and Power Processor for New Millennium's Deep Space 1 Mission," AIAA Paper 97-2778, July 1997.
- ¹⁵Curran, F. M., Peterson, T., and Pencil, E., "Pulse Plasma Thruster Technology Directions," AIAA Paper 97-2926, July 1997.
- ¹⁶Paccani, G., and Chiarotti, U., "Behavior of Quasi-Steady Ablative MPD Thrusters with Different Propellants," International Electric Propulsion Conf., Paper 95-118, Sept. 1995.
- ¹⁷Andrenucci, M., Marcuccio, S., Genovese, A., Bartoli, C., Gonzalez, J., and Saccoccia, G., "FEEP System Study," International Electric Propulsion Conf., Paper 93-156, Sept. 1993.
- ¹⁸Krulle, G., Auweter-Kurtz, M., and Sasoh, A., "Technology and Application Aspects of Applied Field Magnetoplasmadynamic Propulsion," *Journal of Propulsion and Power*, Vol. 14, No. 5, 1998, pp. 754-763.
- ¹⁹Toki, K., Shimizu, Y., and Kuriki, K., "Experiment (EPEX) of a Repetitively Pulsed MPD Thruster Onboard Space Flyer Unit (SFU)," *Proceedings of the 25th International EP Conference*, Electric Rocket Propulsion Society, Columbus, OH, 1997 (IEPC Paper 97-120).
- ²⁰Shtyrlin, A. F., "State of the Art and Future Prospects of Colloidal Electric Thrusters," *Proceedings of the 24th International EP Conference* (Moscow, Russia), 1995 (IEPC Paper 95-103).
- ²¹Landis, G. A., Bailey, S. G., and Piszczor, M. F., "Recent Advances in Solar Cell Technology," AIAA Paper 95-0027, Jan. 1995.
- ²²Jones, P. A., Murphy, D. M., and Piszczor, M. F., "A Linear Reflective Photovoltaic Concentrator Solar Array Flight Experiment," Intersociety Energy Convection Conf., Paper AP-351, Orlando, FL, July 1995.
- ²³Kurland, R., and Stella, P. M., "Advanced Photovoltaic Array Design and Performance," AIAA Paper 92-1058, Feb. 1992.
- ²⁴Anspaugh, B. E., "Solar Cell Radiation Handbook, Addendum 1: 1982-1988," Jet Propulsion Lab., 82-69, California Inst. of Technology, Pasadena, CA, Feb. 1989.
- ²⁵Gussenhoven, M. S., Mullen, E. J., Sperry, M., Kerns, K. J., and Blake, J. B., "The Effect of a March 1991 Storm on Accumulated Dose for Selected Satellite Orbits: CRRES Dose Models," *IEEE Transactions on Nuclear Science*, Vol. 39, No. 6, 1992, pp. 1765-1772.
- ²⁶Guidice, D. A., and Ray, K. P., "PASP Plus Measurements of Space Plasma and Radiation Interactions on Solar Arrays," AIAA Paper 96-0926, Jan. 1996.
- ²⁷Edelbaum, T. N., "Propulsion Requirements for Controllable Satellites," *ARS Journal*, Vol. 31, 1961, pp. 1079-1089.
- ²⁸Samanta Roy, R. I., Hastings, D. E., and Gatsonis, N. A., "A Review of Contamination from Thrusters," AIAA Paper 94-2469, June 1994.
- ²⁹Oh, D. Y., "Computational Modeling of Expanding Plasma Plumes in Space Using a PIC-DSMC Algorithm," Ph.D. Dissertation, Dept. of Aeronautics and Astronautics, Massachusetts Inst. of Technology, Cambridge, MA, Feb. 1997.
- ³⁰Pencil, E. J., Randolph, J., and Manzella, D. H., "End-of-Life Stationary Plasma Thruster Far-Field Plume Characterization" AIAA Paper 96-2709, July 1996.
- ³¹Myers, R. M., Arrington, L. A., Pencil, E. C., Carter, J., Heminger, J., and Gatsonis, N., "Pulsed Plasma Thruster Contamination," AIAA Paper 96-2729, July 1996.
- ³²Sovey, J. S., Carney, L. M., and Knowles, S. C., "Electromagnetic Emission Experiences Using EP Systems," *Journal of Propulsion and Power*, Vol. 5, No. 5, 1989, pp. 534-547.
- ³³Zafran, S., "Arcjet System Integration Development, Final Report," NASA-CR-187147; E-8655; NAS 1.26:187147, March 1994.
- ³⁴Dickens, J. C., Kristiansen, M., and O'Hair, E., "Plume Model of Hall Effect Plasma Thruster, with Temporal Consideration," International Electric Propulsion Conf., Paper 95-171, Sept. 1995.
- ³⁵Pollard, J. E., and Janson, S. W., "Spacecraft Electric Propulsion Applications," The Aerospace Corp., Aerospace Rept. ATR-96 (8201)-1, Feb. 1996.